Letter

Slowest and fastest information scrambling in the strongly disordered XXZ model

Myeonghyeon Kim [1] and Dong-Hee Kim [2,3,*]
[1] Department of Physics and Astronomy, Seoul National University, Seoul 08826, Korea
[2] Department of Physics and Photon Science, Gwangju Institute of Science and Technology, Gwangju 61005, Korea
[3] School of Physics, Korea Institute for Advanced Study, Seoul 02455, Korea

(Received 23 March 2023; revised 12 June 2023; accepted 13 June 2023; published 22 June 2023)

We present a perturbation method to compute the out-of-time-ordered correlator in the strongly disordered Heisenberg XXZ model in the deep many-body localized regime. We characterize the discrete structure of the information propagation across the eigenstates, revealing a highly structured light cone confined by the strictly logarithmic upper and lower bounds representing the slowest and fastest scrambling available in this system. We explain these bounds by deriving the closed-form expression of the effective interaction for the slowest scrambling and by constructing the effective model of a half length for the fastest scrambling. We extend our lowest-order perturbation formulations to the higher dimensions, proposing that the logarithmic upper and lower light cones may persist in a finite two-dimensional system in the limit of strong disorder and weak hopping.

DOI: 10.1103/PhysRevB.107.L220203

Slow scrambling of quantum information is one of the intriguing phenomena occurring in many-body localized (MBL) systems [1–5]. The time scale of scrambling dynamics [6] in MBL systems is distinguished from Anderson localization in noninteracting systems where correlation decays exponentially [7,8] and also from the fast scrambling expected in ideal chaotic systems [9–11]. The logarithmic time scale of information propagation was first reported by the growth of entanglement entropy in the disordered XXZ chain quenched from a product state [12–14], which was explained in the picture of the quasilocal integral of motion (LIOM) [15–18]. The Lieb-Robinson bound indicating the upper bound on information propagation speed was modified accordingly in this picture, proposing the logarithmic light cone (LLC) of the information front moving at a finite speed defined in logarithmic time instead of linear time [19–24].

Despite the numerical evidence of LLC found in MBL systems [24–29], a basic understanding of LLC primarily relies on the effective l-bit Hamiltonian [17,18]. The hypothesized exponentially decaying effective interaction $J_{\text{eff}}(r) \propto \exp(-r/\xi)$ acting on two remote LIOMs at distance r with a decay length ξ is a key to interpreting the time scale $t \sim 1/J_{\text{eff}}$ exponentially increasing with r. Although this is well established to describe the dephasing dynamics in one dimension (1D), the effective picture lacks the system-specific details that can still be necessary for understanding of the phenomena in a particular system. In the simple setting with a fixed ξ, the slope of LLC is given by ξ^{-1} [20]. However, as noted in the construction of the l-bit model [18], J_{eff} and ξ generally vary with eigenstates as well as disorder configurations. We study the consequence of such dependence in characterizing information scrambling in the disordered XXZ model in the deep MBL regime.

On the other hand, practical signatures of MBL in two dimensions (2D) have attracted much attention theoretically [28–43] and experimentally [44–46] at finite systems, while it has been argued that 2D MBL is asymptotically unstable toward the avalanche of rare thermal regions [47–51]. In particular, the evidence of LIOMs [34] and LLC [29] has been recently presented in higher dimensions by the numerical construction of the l-bit Hamiltonian. These motivate us to revisit the computation of the out-of-time-ordered correlator (OTOC) [6], a diagnostic tool for information scrambling, for characterization beyond the generic l-bit description both in 1D and 2D.

In this Letter, we develop a perturbation formulation of OTOC in the strongly disordered XXZ model in the weak hopping limit. Measuring OTOC for each eigenstate, we reveal the discrete structure of the light cone built by the allowed lowest orders of perturbation varying with the intervening spin states at a given r. Remarkably, the light cone is bounded by the two logarithmic slopes representing the slowest and fastest scrambling. We derive an analytic formula for the effective interaction for the slowest scrambling and describe the fastest scrambling by the half-length effective Ising chain. Extending our method to 2D, we demonstrate the logarithmic light cones of the slowest and fastest scrambling in 2D within the lowest-order perturbation formulations.

For perturbation expansion, we decompose the XXZ Hamiltonian as $\hat{H} \equiv \hat{H}_0 + \hat{V}$, where the unperturbed part $\hat{H}_0$ and the hopping perturbation $\hat{V}$ are given as

$$\hat{H}_0 = \frac{J_z}{2}\sum_i \hat{\sigma}_i^z \hat{\sigma}_{i+1}^z + \sum_i h_i \hat{\sigma}_i^z, \tag{1}$$

$$\hat{V} = J\sum_i (\hat{\sigma}_i^+ \hat{\sigma}_{i+1}^- + \hat{\sigma}_i^- \hat{\sigma}_{i+1}^+). \tag{2}$$

The random disorder field is drawn from the uniform distribution of $h_i \in [-h, h]$. We assume that the unperturbed

*donghekim@gist.ac.kr

state is nondegenerate and localized in the Fock space of the $\hat{\sigma}_z$-basis states. We consider the strong disorder and weak hopping limit of $J \ll J_z \ll h$ in the deep MBL regime. We compute the perturbation corrections in energy within the Rayleigh-Schrödinger perturbation theory using multiprecision numerics to handle strong cancellations and critical round-off errors (see Supplemental Material [52] and references [53–56] therein).

We define OTOC by the squared commutator of two $\hat{\sigma}_x$ operators initially located at a and b as

$$C_\alpha(r,t) = \tfrac{1}{2}\langle\alpha|\left|\left[\hat{\sigma}_a^x(t), \hat{\sigma}_b^x\right]\right|^2|\alpha\rangle = 1 - \mathrm{Re}[F_\alpha(r,t)], \quad (3)$$

where the correlator $F_\alpha(r,t) = \langle\alpha|\hat{\sigma}_a^x(t)\hat{\sigma}_b^x\hat{\sigma}_a^x(t)\hat{\sigma}_b^x|\alpha\rangle$ and $r \equiv |a-b| - 1 \geqslant 0$ is the separation between a and b. Choosing $|\alpha\rangle$ to be an eigenstate, the correlator can be approximated at weak perturbation as

$$F_\alpha(r,t) = \sum_{\beta,\gamma,\delta} s_{\alpha\beta\gamma\delta} e^{i\Omega_{\alpha\beta\gamma\delta}t} \approx \exp\left(iJ_{\mathrm{eff}}^\alpha t\right), \quad (4)$$

where the frequency $\Omega_{\alpha\beta\gamma\delta} = E_\alpha - E_\beta + E_\gamma - E_\delta$ and the coefficient $s_{\alpha\beta\gamma\delta} = \langle\alpha|\hat{\sigma}_a^x|\beta\rangle\langle\beta|\hat{\sigma}_b^x|\gamma\rangle\langle\gamma|\hat{\sigma}_a^x|\delta\rangle\langle\delta|\hat{\sigma}_b^x|\alpha\rangle$. Assuming that a perturbation correction in a state vector is small, the single dominant term is found at $s_{\alpha\beta\gamma\delta} \approx 1$ for $|\alpha\rangle \approx |\alpha^{(0)}\rangle$, $|\beta\rangle \approx |\beta^{(0)}\rangle = \hat{\sigma}_a^x|\alpha^{(0)}\rangle$, $|\gamma\rangle \approx |\gamma^{(0)}\rangle = \hat{\sigma}_b^x\hat{\sigma}_a^x|\alpha^{(0)}\rangle$, and $|\delta\rangle \approx |\delta^{(0)}\rangle = \hat{\sigma}_b^x|\alpha^{(0)}\rangle$, where the superscript denotes the corresponding unperturbed state. The frequency of the dominant component is rewritten in terms of the perturbation corrections as

$$J_{\mathrm{eff}}^\alpha = \Delta E_\alpha - \Delta E_\beta + \Delta E_\gamma - \Delta E_\delta, \quad (5)$$

which we referred to as an effective interaction from the analogy to the one in $F(t) = \exp(\pm 4iJ_{\mathrm{eff}}t)$ given for the effective l-bit model [20–24]. The same expression of J_{eff}^α can also be extracted using the protocol of the double electron-electron resonance (DEER) [57–60]. From Eqs. (3) and (4), the disorder average of C_α is written as

$$\langle C_\alpha(r,t)\rangle_{\mathrm{av}} \approx 1 - \mathrm{Re}\left[\int_{-\infty}^{\infty} e^{iJ_{\mathrm{eff}}^\alpha t} P\left(J_{\mathrm{eff}}^\alpha\right) dJ_{\mathrm{eff}}^\alpha\right], \quad (6)$$

with the probability distribution $P(J_{\mathrm{eff}}^\alpha)$ being obtained by computing J_{eff}^α for random disorder configurations. In this weak perturbation formulation, only the energy corrections are important while the small corrections in the state vectors are irrelevant. Measuring OTOC in the Fock space with $|\alpha^{(0)}\rangle$ leads to the same expression.

Figure 1 displays the scrambling time t^* as a function of r obtained by solving $\langle C_\alpha(r,t^*)\rangle_{\mathrm{av}} = 0.5$ for each eigenstate. It turns out that t^* is not on a single light cone but structured by the lowest order of the nonvanishing perturbation term in Eq. (5), varying with the intervening spin configuration in $|\alpha^{(0)}\rangle$. The lowest order $n_\alpha(r)$ is determined by the minimum number of the hopping operators flipping all intervening spins, which is written as $n_\alpha(r) = 2(r - m_s^\alpha)$, where m_s^α is the number of staggered spin pairs found in $|\alpha^{(0)}\rangle$ between a and b.

Remarkably, the discrete structure of t^* indicates the sharp upper and lower bounds in the logarithmic slope, representing the slowest and fastest scrambling available in this system. These bounds correspond to $J_{\mathrm{eff}}^\alpha \propto J^{2r}$ ($m_s^\alpha = 0$) and $J_{\mathrm{eff}}^\alpha \propto J^r$ ($m_s^\alpha = r/2$) at even r, which are associated with $|\alpha^{(0)}\rangle$ of the

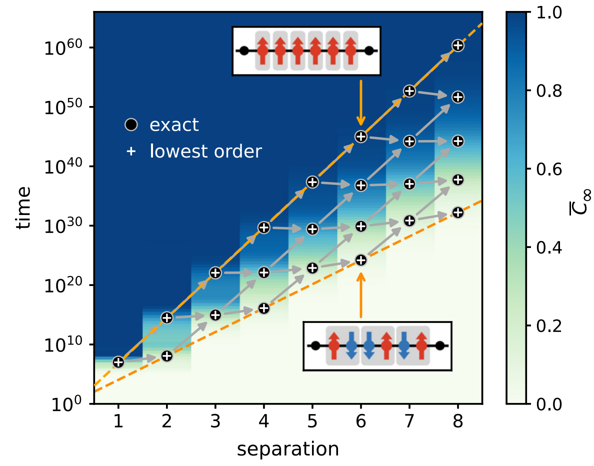

FIG. 1. Light cone structure of the disordered XXZ chain in the deep MBL regime. The markers denote the scrambling time $J_z t^*$ obtained at the fixed value of the disorder-averaged OTOC $\langle C_\alpha(r,t^*)\rangle_{\mathrm{av}} = 0.5$ for each eigenstate α, comparing the lowest-order perturbation results with the exact diagonalization at $J/J_z = 0.001$ and $h/J_z = 10$. The arrows indicate the allowed change of t^* with increasing separation. The background color indicates the infinite-temperature OTOC $\overline{C}_\infty$, the average of $\langle C_\alpha(r,t)\rangle_{\mathrm{av}}$ over all eigenstates.

ferromagnetic (FM) domain and the chain of staggered spin pairs such as in the antiferromagnetic (AF) state, respectively. This structure is hidden in the infinite-temperature OTOC, an average over the eigenstates, revealing the detailed view of the light cone in the strongly disordered XXZ model.

For the slowest scrambling, we obtain the lowest-order expression of $J_{\mathrm{eff}}^{\mathrm{FM}}$ at the FM unperturbed state as

$$J_{\mathrm{eff}}^{\mathrm{FM}} = 2J_z\left(\frac{J}{2}\right)^{2r} \sum_{k=0}^{r} F_k^2 \frac{A_k + B_{k+1}}{A_k + B_{k+1} - J_z} G_{k+1}^2, \quad (7)$$

where $A_k = h_a - h_{a+k}$ and $B_k = h_b - h_{a+k}$. The factors are given as $F_k = \prod_{j=1}^{k} A_j^{-1}$ and $G_k = \prod_{j=k}^{r} B_j^{-1}$, where an empty product is unity. Note that a nonzero interaction J_z is essential. While the detailed derivation is provided in the Supplemental Material [52], each term is conceptually illustrated in Fig. 2(a). The diagrams of ΔE_β and ΔE_δ describe the lowest order of $\hat{V}$ that moves an excitation site by site to sweep through the intervening FM area and ΔE_γ includes all such hopping configurations with two excitations.

The fastest scrambling in the lowest-order picture is described by a half number of pseudospins each of which maps to a two-site block of a staggered spin pair as sketched in Fig. 2(b). The lowest order is given by the $r/2$ number of the $\hat{V}$ operators applying exclusively on each block for the simultaneous flip of the two opposite spins. The resulting two-level structure leads us to define the pseudospin Pauli operators $\hat{X}$ and $\hat{Z}$ in the basis of $|\Uparrow\rangle \equiv |\downarrow\uparrow\rangle$ and $|\Downarrow\rangle \equiv |\uparrow\downarrow\rangle$ for the reduced Hilbert space. We choose the AF state to evaluate $J_{\mathrm{eff}}^{\mathrm{AF}}$, but all configurations filled up with staggered spin pairs provide the equivalent results.

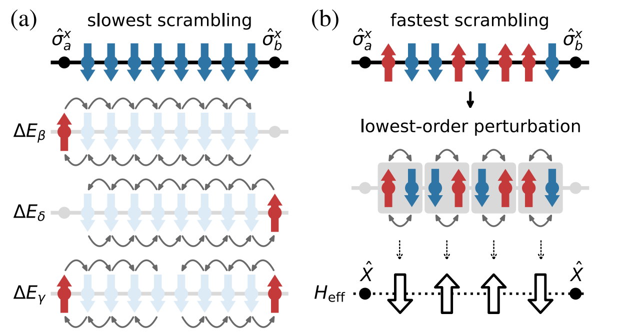

FIG. 2. Schematic diagrams of the lowest-order contributions to the effective interactions. (a) In the slowest scrambling, the lowest order is given by the minimum sequential moves of the excitation covering the intervening spin-polarized region. (b) In the fastest scrambling across the blocks of staggered spin pairs, the lowest order only involves spin exchanges within the block, mapping the block into one Ising pseudospin.

At the lowest order, $J_{\rm eff}^{\rm AF}$ in the XXZ chain is exactly reproduced by the Ising chain of a half length $l = r/2$,

$$\hat{H}_{\rm Ising} = -\frac{J_z}{2}\sum_{k=0}^{l}\hat{Z}_k\hat{Z}_{k+1} + \sum_{k=0}^{l+1}\Delta_k\hat{Z}_k + J\sum_{k=1}^{l}\hat{X}_k, \quad (8)$$

where $\Delta_0 = h_a$, $\Delta_{l+1} = -h_b$, and $\Delta_k = h_{a+2k} - h_{a+2k-1}$ for $k = 1, \dots, l$. The perturbation part is $J\sum_i \hat{X}_i$. The FM state corresponds to the AF state of the XXZ chain and $\hat{X}_{0,l+1}$ replaces $\hat{\sigma}^x_{a,b}$ for the OTOC operators. While we cannot find an analytic formula of $J_{\rm eff}^{\rm AF}$, the half length chain significantly reduces the numerical cost for the full perturbation calculation [52]. Since nonzero J_z is essential in both $J_{\rm eff}^{\rm FM}$ and $J_{\rm eff}^{\rm AF}$, hereafter we express the quantities in a dimensionless form as $\tilde{t} \equiv J_z t$, $\tilde{h} \equiv h/J_z$, $\tilde{J} \equiv J/J_z$, and $\tilde{J}_{\rm eff} \equiv J_{\rm eff}/J_z$.

Figure 3 presents the numerical results based on Eqs. (7) and (8), which verifies the logarithmic propagation of the fronts of the slowest and fastest scrambling but also examines the decay length scale of the effective interaction. The disorder-averaged OTOC plotted as a function of $r^{-1}\ln\tilde{t}$ exhibits an increase that gets sharper as r increases, assuring the strictly logarithmic slopes of the light cone. The shift $g \equiv q\ln\tilde{J}$ comes from $\tilde{J}_{\rm eff} \propto \tilde{J}^{qr}$, where $q = 2(1)$ is for the FM(AF) state.

Assuming the form of $\tilde{J}_{\rm eff} \sim \exp(-r/\xi)$, we extract the inverse decay length as $\xi^{-1} = -r^{-1}\ln|\tilde{J}_{\rm eff}|$. The distribution of ξ^{-1} is increasingly peaked as r increases, indicating a well-defined $\langle\xi^{-1}\rangle_{\rm av}$. The skewed shape that we observe here at the particular states is different from the log-normal shape previously reported at infinite temperature [59]. In addition, we find that $\langle\xi^{-1}\rangle_{\rm av}$ follows the characteristic behavior with varying parameters as

$$\langle\xi^{-1}\rangle_{\rm av} = -\frac{\langle\ln|\tilde{J}_{\rm eff}|\rangle_{\rm av}}{r} \sim \begin{cases}\ln(\tilde{h}/\tilde{J})^2 & \text{for FM,}\\ \ln(\tilde{h}^{\kappa}/\tilde{J}) & \text{for AF.}\end{cases} \quad (9)$$

One can directly extract the behavior for the FM state from Eq. (7) giving $\tilde{J}_{\rm eff}^{\rm FM} \sim (\tilde{J}/2\tilde{h})^{2r}$ after rewriting it in the dimensionless form. For the AF state, we determine the exponent $\kappa \approx 1.55$ numerically.

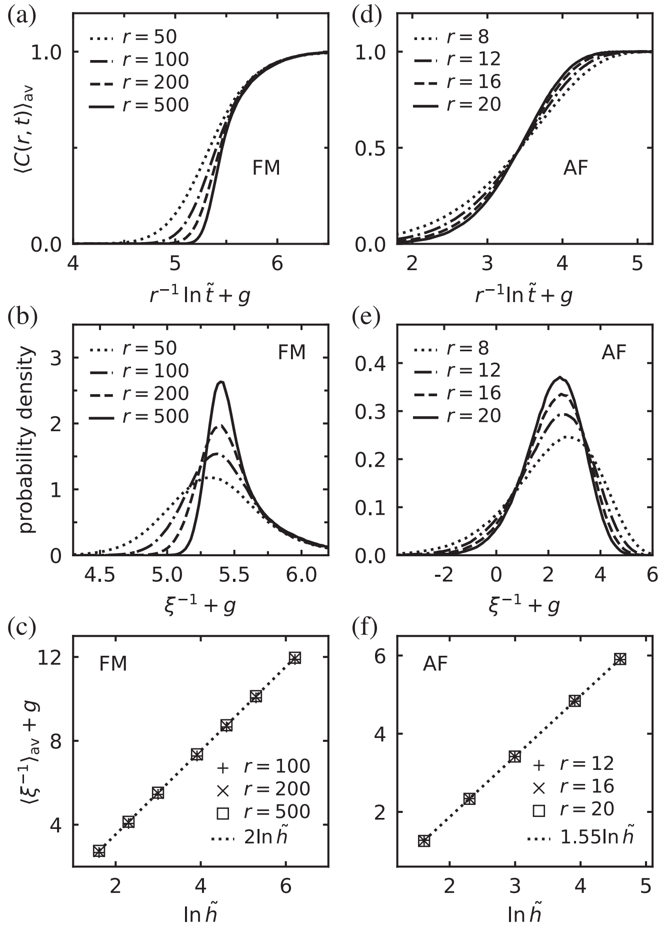

FIG. 3. Slowest and fastest scrambling in the lowest-order perturbation theory for the strongly disordered XXZ chain. The disorder average $\langle C(r,t)\rangle_{\rm av}$, the distribution of $\xi^{-1} \equiv -r^{-1}\ln|\tilde{J}_{\rm eff}|$, and the decay length $\langle\xi^{-1}\rangle_{\rm av}$ are computed at $h/J_z = 20$ for the (a)–(c) FM and (d)–(f) AF states. The constant g is set to be $2\ln\tilde{J}$ (FM) and $\ln\tilde{J}$ (AF).

Our lowest-order formulations developed above in 1D can be readily extended to 2D by considering the multiple paths of the same Manhattan distance between the two sites **a** and **b**, namely the number of edges to hop along the path, composing the nonvanishing lowest-order terms. Below we describe the calculations of $J_{\rm eff}$ at the FM and AF states in $L_x \times L_y$ lattices with the two operators being located at the opposite corners as sketched in Fig. 4. We remove boundary artifacts by adding the FM or AF environments to the system.

For the FM state, the lowest order is determined as $2r(\mathbf{a},\mathbf{b}) = 2(L_x + L_y - 3)$, which depends on the number of sites along the shortest paths between **a** and **b**. The 2D variant of Eq. (7) is written in a dimensionless form as

$$\tilde{J}_{\rm eff}^{\rm FM} = 2\left(\frac{\tilde{J}}{2\tilde{h}}\right)^{2r}\sum_{(\mathbf{x}_1\to\mathbf{x}_2)}{}' \tilde{F}_{\mathbf{x}_1}^2\frac{\tilde{A}_{\mathbf{x}_1} + \tilde{B}_{\mathbf{x}_2}}{\tilde{A}_{\mathbf{x}_1} + \tilde{B}_{\mathbf{x}_2} - \tilde{h}^{-1}}\tilde{G}_{\mathbf{x}_2}^2, \quad (10)$$

where $\tilde{A}_{\mathbf{x}} = (\tilde{h}_{\mathbf{a}} - \tilde{h}_{\mathbf{x}})/\tilde{h}$ and $\tilde{B}_{\mathbf{x}} = (\tilde{h}_{\mathbf{b}} - \tilde{h}_{\mathbf{x}})/\tilde{h}$. The primed sum runs over directed links $(\mathbf{x}_1 \to \mathbf{x}_2)$ on any shortest path

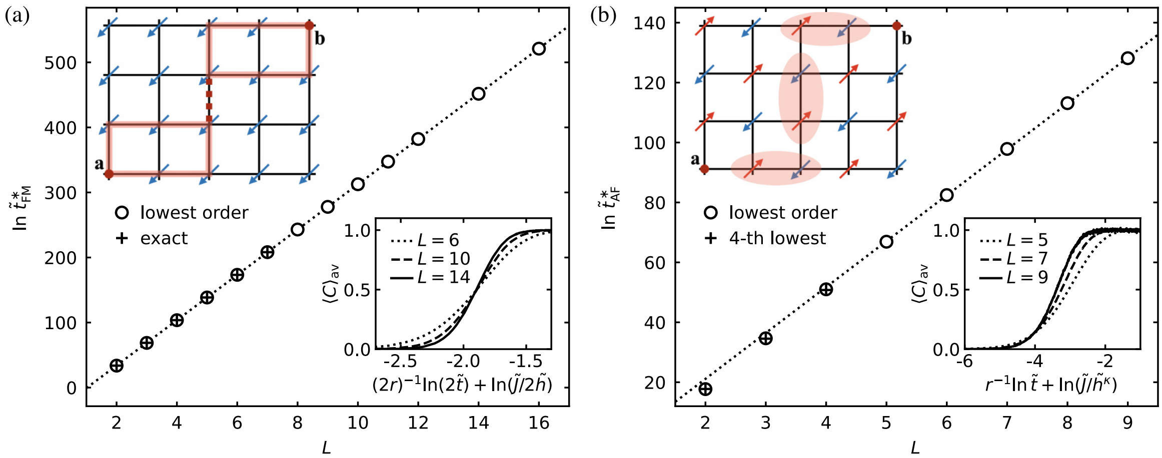

FIG. 4. Logarithmic light cones in the 2D strongly disordered XXZ model. The scrambling time t^* is computed at $J/J_z = 0.001$ and $h/J_z = 20$ for the (a) FM and (b) AF states, corresponding to the slowest and fastest scrambling, respectively. In the $(L+1)\times L$ lattices, the $\hat{\sigma}_x$ operators of OTOC are located at the diagonal corners with separation $r = 2(L-1)$. The schematic diagram in the insets shows an example of a path contributing to the lowest-order perturbation calculation.

from **a** to **b**. The factors $\tilde{F}$ and $\tilde{G}$ are defined as

$$\tilde{F}_{\mathbf{x}} = \sum_{w(\mathbf{a},\mathbf{x})} \prod_{\mathbf{y}\in w}^{\mathbf{a}} \tilde{A}_{\mathbf{y}}^{-1}, \quad \tilde{G}_{\mathbf{x}} = \sum_{w(\mathbf{b},\mathbf{x})} \prod_{\mathbf{y}\in w}^{\mathbf{b}} \tilde{B}_{\mathbf{y}}^{-1},$$

where the sum runs over every shortest path $w(\mathbf{x}_0, \mathbf{x})$ connecting $\mathbf{x}_0$ and $\mathbf{x}$ and $\prod^{\mathbf{a}(\mathbf{b})}$ excludes $\mathbf{a}(\mathbf{b})$ in the product over every site $\mathbf{y}$ along the path w. The squared factors consider the excitation moving forward and backward along different paths unlike in 1D.

For the AF state, we consider $(L+1)\times L$ lattices, where $l \equiv L-1$ pairs of the up-and-down spins exist along any shortest path between **a** and **b**, giving the lowest order $r = 2l$. Unlike the FM case, the lowest-order contributions can be separated into each path because a string of the hopping operators for paired spin flips must stay on the same path. For a path $w \equiv (\mathbf{a}, \mathbf{x}_1, \mathbf{x}_2, \dots, \mathbf{x}_{2l}, \mathbf{b})$, the contribution is then given by the Ising chain with path-dependent parameters, which can be expressed as $\hat{H}_{\rm Ising}[\mathbf{\Delta}(w)]$ with $\Delta_0 = h_{\mathbf{a}}$, $\Delta_{l+1} = -h_{\mathbf{b}}$, and $\Delta_k = h_{\mathbf{x}_{2k}} - h_{\mathbf{x}_{2k-1}} + 2J$, where $2J$ is from the AF surroundings. Summing over all paths, we write $\tilde{J}^{\rm AF}_{\rm eff}$ as

$$\tilde{J}^{\rm AF}_{\rm eff}(\mathbf{a}, \mathbf{b}) = \sum_{w} \tilde{J}^{\rm AF}_{\rm eff}[\hat{H}_{\rm Ising}[\mathbf{\Delta}(w)]], \qquad (11)$$

which involves an exponentially growing number of terms as L increases but allows us to go well beyond the system-size limit of the exact diagonalization and the numerical perturbation calculations for arbitrary orders.

Figure 4 shows 2D LLCs from the scrambling time and the disorder-averaged OTOC measured at the FM and AF states in the 2D XXZ model in the strong disorder and weak hopping limit. Since the number of the shortest paths scales as 4^l, a rough estimate ignoring disorder correlations between the paths suggests $\tilde{J}^{\rm AF}_{\rm eff} \sim 4^l e^{-2l/\xi}$ from Eq. (11), implying LLC for $\langle \xi^{-1}\rangle_{\rm av} \gg \ln 2$. While our calculations are based on the lowest-order perturbation theory, the numerical tests show excellent agreement with the exact diagonalization at small L's for the FM state and with the full perturbation calculations up to the fourth lowest order for the AF state. Our observation of LLC in the strongly disordered XXZ model is also consistent with the previous evidence of LLC reported in the 2D bosonic system with the l-bit construction at the strong disorder and weak interaction limit [29].

In conclusion, our perturbation formulation reveals the peculiar structure of slow information propagation in the paradigmatic XXZ model in the deep MBL regime. The slowest and fastest scrambling identified in the discrete structure of OTOC characterizes the drastic difference between the spin-polarized and the Néel states of the intervening spins prepared for the OTOC or DEER measurements. We have derived the closed-form expression of the effective interaction for the slowest scrambling and found the effective Ising chain of a half length describing the fastest scrambling, presenting the sharp logarithmic upper and lower bounds of the light cone.

Our observation of LLCs extends the variety of the practical MBL signatures previously reported in finite 2D systems, although the instability of 2D MBL in the asymptotic limit goes beyond our method. A challenging direction for future study may include the behavior of OTOC measured across 2D thermal defects and its finite-size effects. On the other hand, our findings on the distance effectively reduced by half at the fastest scrambling imply an interesting question on its l-bit representation. In contrast to the slowest one, the fastest scrambling involves only the half number of the pseudospins, proposing to further explore how the mapping to the l-bit Hamiltonian encodes these system-specific scrambling structures for the XXZ model.

This work was supported from the Basic Science Research Program through the National Research Foundation of Korea (Grant No. NRF-2017R1D1A1B03034669) and also from a GIST Research Institute (GRI) grant funded by the GIST. We appreciate APCTP for its hospitality during the completion of this work.

[1] R. Nandkishore and D. A. Huse, Many body localization and thermalization in quantum statistical mechanics, Annu. Rev. Condens. Matter Phys. **6**, 15 (2015).
[2] F. Alet and N. Laflorencie, Many-body localization: An introduction and selected topics, C. R. Phys. **19**, 498 (2018).
[3] S. A. Parameswaran and R. Vasseur, Many-body localization, symmetry and topology, Rep. Prog. Phys. **81**, 082501 (2018).
[4] D. A. Abanin, E. Altman, I. Bloch, and M. Serbyn, Colloquium: Many-body localization, thermalization, and entanglement, Rev. Mod. Phys. **91**, 021001 (2019).
[5] S. Gopalakrishnan and S. A. Parameswaran, Dynamics and transport at the threshold of many-body localization, Phys. Rep. **862**, 1 (2020).
[6] S. Xu and B. Swingle, Scrambling dynamics and out-of-time-ordered correlators in quantum many-body systems: A tutorial, arXiv:2202.07060.
[7] C. K. Burrell and T. J. Osborne, Bounds on the Speed of Information Propagation in Disordered Quantum Spin Chains, Phys. Rev. Lett. **99**, 167201 (2007).
[8] E. Hamza, R. Sims, and G. Stolz, Dynamical localization in disordered quantum spin systems, Commun. Math. Phys. **315**, 215 (2012).
[9] J. Maldacena, S. H. Shenker, and D. Stanford, A bound on chaos, J. High Energ. Phys. 08 (2016) 106.
[10] D. A. Roberts and B. Swingle, Lieb-Robinson Bound and the Butterfly Effect in Quantum Field Theories, Phys. Rev. Lett. **117**, 091602 (2016).
[11] Y. Gu, X.-L. Qi, and D. Stanford, Local criticality, diffusion and chaos in generalized Sachdev-Ye-Kitaev models, J. High Energ. Phys. 05 (2017) 125.
[12] G. D. Chiara, S. Montangero, P. Calabrese, and R. Fazio, Entanglement entropy dynamics of Heisenberg chains, J. Stat. Mech. (2006) P03001.
[13] M. Žnidarič, T. Prosen, and P. Prelovšek, Many-body localization in the Heisenberg XXZ magnet in a random field, Phys. Rev. B **77**, 064426 (2008).
[14] J. H. Bardarson, F. Pollmann, and J. E. Moore, Unbounded Growth of Entanglement in Models of Many-Body Localization, Phys. Rev. Lett. **109**, 017202 (2012).
[15] M. Serbyn, Z. Papić, and D. A. Abanin, Universal Slow Growth of Entanglement in Interacting Strongly Disordered Systems, Phys. Rev. Lett. **110**, 260601 (2013).
[16] R. Vosk and E. Altman, Many-Body Localization in One Dimension as a Dynamical Renormalization Group Fixed Point, Phys. Rev. Lett. **110**, 067204 (2013).
[17] M. Serbyn, Z. Papić, and D. A. Abanin, Local Conservation Laws and the Structure of the Many-Body Localized States, Phys. Rev. Lett. **111**, 127201 (2013).
[18] D. A. Huse, R. Nandkishore, and V. Oganesyan, Phenomenology of fully many-body-localized systems, Phys. Rev. B **90**, 174202 (2014).
[19] I. H. Kim, A. Chandran, and D. A. Abanin, Local integrals of motion and the logarithmic lightcone in many-body localized systems, arXiv:1412.3073.
[20] R. Fan, P. Zhang, H. Shen, and H. Zhai, Out-of-time-order correlation for many-body localization, Sci. Bull. **62**, 707 (2017).
[21] B. Swingle and D. Chowdhury, Slow scrambling in disordered quantum systems, Phys. Rev. B **95**, 060201(R) (2017).
[22] Y. Chen, Universal logarithmic scrambling in many body localization, arXiv:1608.02765.
[23] X. Chen, T. Zhou, D. A. Huse, and E. Fradkin, Out-of-time-order correlations in many-body localized and thermal phases, Ann. Phys. (Berlin) **529**, 1600332 (2017).
[24] R.-Q. He and Z.-Y. Lu, Characterizing many-body localization by out-of-time-ordered correlation, Phys. Rev. B **95**, 054201 (2017).
[25] D.-L. Deng, X. Li, J. H. Pixley, Y.-L. Wu, and S. Das Sarma, Logarithmic entanglement lightcone in many-body localized systems, Phys. Rev. B **95**, 024202 (2017).
[26] Y. Huang, Y.-L. Zhang, and X. Chen, Out-of-time-ordered correlators in many-body localized systems, Ann. Phys. (Berlin) **529**, 1600318 (2017).
[27] M. C. Bañuls, N. Y. Yao, S. Choi, M. D. Lukin, and J. I. Cirac, Dynamics of quantum information in many-body localized systems, Phys. Rev. B **96**, 174201 (2017).
[28] G. De Tomasi, F. Pollmann, and M. Heyl, Efficiently solving the dynamics of many-body localized systems at strong disorder, Phys. Rev. B **99**, 241114(R) (2019).
[29] S. W. Kim, G. De Tomasi, and M. Heyl, Real-time dynamics of one-dimensional and two-dimensional bosonic quantum matter deep in the many-body localized phase, Phys. Rev. B **104**, 144205 (2021).
[30] T. B. Wahl, A. Pal, and S. H. Simon, Signatures of the many-body localized regime in two dimensions, Nat. Phys. **15**, 164 (2019).
[31] A. Kshetrimayum, M. Goihl, and J. Eisert, Time evolution of many-body localized systems in two spatial dimensions, Phys. Rev. B **102**, 235132 (2020).
[32] H. Théveniaut, Z. Lan, G. Meyer, and F. Alet, Transition to a many-body localized regime in a two-dimensional disordered quantum dimer model, Phys. Rev. Res. **2**, 033154 (2020).
[33] A. Szabó and U. Schneider, Mixed spectra and partially extended states in a two-dimensional quasiperiodic model, Phys. Rev. B **101**, 014205 (2020).
[34] E. Chertkov, B. Villalonga, and B. K. Clark, Numerical Evidence for Many-Body Localization in Two and Three Dimensions, Phys. Rev. Lett. **126**, 180602 (2021).
[35] F. Pietracaprina and F. Alet, Probing many-body localization in a disordered quantum dimer model on the honeycomb lattice, SciPost Phys. **10**, 044 (2021).
[36] K. S. C. Decker, D. M. Kennes, and C. Karrasch, Many-body localization and the area law in two dimensions, Phys. Rev. B **106**, L180201 (2022).
[37] E. V. H. Doggen, I. V. Gornyi, and D. G. Polyakov, Many-body localization in a tilted potential in two dimensions, Phys. Rev. B **105**, 134204 (2022).
[38] U. Agrawal, R. Vasseur, and S. Gopalakrishnan, Quasiperiodic many-body localization transition in dimension $d > 1$, Phys. Rev. B **106**, 094206 (2022).
[39] A. Štrkalj, E. V. H. Doggen, and C. Castelnovo, Coexistence of localization and transport in many-body two-dimensional Aubry-André models, Phys. Rev. B **106**, 184209 (2022).
[40] H.-K. Tang, N. Swain, D. C. W. Foo, B. J. J. Khor, G. Lemarié, F. F. Assaad, S. Adam, and P. Sengupta, Evidence of many-body localization in *2D* from quantum Monte Carlo simulation, arXiv:2106.08587.
[41] J. Li, A. Chan, and T. B. Wahl, Fermionic quantum circuits reproduce experimental two-dimensional many-body localization transition point, arXiv:2108.08268.

[42] D. C. W. Foo, N. Swain, P. Sengupta, G. Lemarié, and S. Adam, A stabilization mechanism for many-body localization in two dimensions, arXiv:2202.09072.

[43] F. Venn, T. B. Wahl, and B. Béri, Many-body-localization protection of eigenstate topological order in two dimensions, arXiv:2212.09775.

[44] J.-Y. Choi, S. Hild, J. Zeiher, P. Schauß, A. Rubio-Abadal, T. Yefsah, V. Khemani, D. A. Huse, I. Bloch, and C. Gross, Exploring the many-body localization transition in two dimensions, Science **352**, 1547 (2016).

[45] S. S. Kondov, W. R. McGehee, W. Xu, and B. DeMarco, Disorder-Induced Localization in a Strongly Correlated Atomic Hubbard Gas, Phys. Rev. Lett. **114**, 083002 (2015).

[46] P. Bordia, H. Lüschen, S. Scherg, S. Gopalakrishnan, M. Knap, U. Schneider, and I. Bloch, Probing Slow Relaxation and Many-Body Localization in Two-Dimensional Quasiperiodic Systems, Phys. Rev. X **7**, 041047 (2017).

[47] W. De Roeck and F. Huveneers, Stability and instability towards delocalization in many-body localization systems, Phys. Rev. B **95**, 155129 (2017).

[48] W. De Roeck and J. Z. Imbrie, Many-body localization: Stability and instability, Philos. Trans. R. Soc. A **375**, 20160422 (2017).

[49] I.-D. Potirniche, S. Banerjee, and E. Altman, Exploration of the stability of many-body localization in $d > 1$, Phys. Rev. B **99**, 205149 (2019).

[50] S. Gopalakrishnan and D. A. Huse, Instability of many-body localized systems as a phase transition in a nonstandard thermodynamic limit, Phys. Rev. B **99**, 134305 (2019).

[51] E. V. H. Doggen, I. V. Gornyi, A. D. Mirlin, and D. G. Polyakov, Slow Many-Body Delocalization beyond One Dimension, Phys. Rev. Lett. **125**, 155701 (2020).

[52] See Supplemental Material at http://link.aps.org/supplemental/10.1103/PhysRevB.107.L220203 for calculation details.

[53] T. Kato, On the convergence of the perturbation method. I, Prog. Theor. Phys. **4**, 514 (1949).

[54] C. Bloch, Sur la théorie des perturbations des états liés, Nucl. Phys. **6**, 329 (1958).

[55] R. Huby, Formulae for non-degenerate Rayleigh-Schrödinger perturbation theory in any order, Proc. Phys. Soc. **78**, 529 (1961).

[56] H. J. Silverstone and T. T. Holloway, Explicit formulas for the Nth-order wavefunction and energy in nondegenerate Rayleigh-Schrödinger perturbation theory, J. Chem. Phys. **52**, 1472 (1970).

[57] M. Serbyn, M. Knap, S. Gopalakrishnan, Z. Papić, N. Y. Yao, C. R. Laumann, D. A. Abanin, M. D. Lukin, and E. A. Demler, Interferometric Probes of Many-Body Localization, Phys. Rev. Lett. **113**, 147204 (2014).

[58] G. Kucsko, S. Choi, J. Choi, P. C. Maurer, H. Zhou, R. Landig, H. Sumiya, S. Onoda, J. Isoya, F. Jelezko, E. Demler, N. Y. Yao, and M. D. Lukin, Critical Thermalization of a Disordered Dipolar Spin System in Diamond, Phys. Rev. Lett. **121**, 023601 (2018).

[59] V. K. Varma, A. Raj, S. Gopalakrishnan, V. Oganesyan, and D. Pekker, Length scales in the many-body localized phase and their spectral signatures, Phys. Rev. B **100**, 115136 (2019).

[60] B. Chiaro, C. Neill, A. Bohrdt, M. Filippone, F. Arute, K. Arya, R. Babbush, D. Bacon, J. Bardin, R. Barends, S. Boixo, D. Buell, B. Burkett, Y. Chen, Z. Chen, R. Collins, A. Dunsworth, E. Farhi, A. Fowler, B. Foxen *et al.*, Direct measurement of nonlocal interactions in the many-body localized phase, Phys. Rev. Res. **4**, 013148 (2022).